Am J Physiol Lung Cell Mol Physiol 318: L1198–L1210, 2020.
First published April 22, 2020; doi:10.1152/ajplung.00063.2020.

RESEARCH ARTICLE

Alveolar heparan sulfate shedding impedes recovery from bleomycin-induced lung injury

W. B. LaRivière,[1,2,3]* S. Liao,[3]* S. A. McMurtry,[3] K. Oshima,[3] X. Han,[4] F. Zhang,[4] S. Yan,[3,5] S. M. Haeger,[1,2,3] M. Ransom,[3] J. A. Bastarache,[6] R. J. Linhardt,[4] E. P. Schmidt,[2,3,7] and Y. Yang[3]

[1]*Medical Scientist Training Program, University of Colorado School of Medicine, Aurora, Colorado;* [2]*Department of Pharmacology, University of Colorado School of Medicine, Aurora, Colorado;* [3]*Department of Medicine, University of Colorado School of Medicine, Aurora, Colorado;* [4]*Department of Chemistry, Rensselaer Polytechnic Institute, Troy, New York;* [5]*College of Life Sciences, Henan Normal University, Xinxiang, China;* [6]*Department of Medicine, Vanderbilt University Medical Center, Nashville, Tennessee; and* [7]*Department of Medicine, Denver Health Medical Center, Denver, Colorado*

Submitted 24 February 2020; accepted in final form 16 April 2020

LaRivière WB, Liao S, McMurtry SA, Oshima K, Han X, Zhang F, Yan S, Haeger SM, Ransom M, Bastarache JA, Linhardt RJ, Schmidt EP, Yang Y. Alveolar heparan sulfate shedding impedes recovery from bleomycin-induced lung injury. *Am J Physiol Lung Cell Mol Physiol* 318: L1198–L1210, 2020. First published April 22, 2020; doi:10.1152/ajplung.00063.2020.—The pulmonary epithelial glycocalyx, an anionic cell surface layer enriched in glycosaminoglycans such as heparan sulfate and chondroitin sulfate, contributes to the alveolar barrier. Direct injury to the pulmonary epithelium induces shedding of heparan sulfate into the air space; the impact of this shedding on recovery after lung injury is unknown. Using mass spectrometry, we found that heparan sulfate was shed into the air space for up to 3 wk after intratracheal bleomycin-induced lung injury and coincided with induction of matrix metalloproteinases (MMPs), including MMP2. Delayed inhibition of metalloproteinases, beginning 7 days after bleomycin using the nonspecific MMP inhibitor doxycycline, attenuated heparan sulfate shedding and improved lung function, suggesting that heparan sulfate shedding may impair lung recovery. While we also observed an increase in air space heparanase activity after bleomycin, pharmacological and transgenic inhibition of heparanase in vivo failed to attenuate heparan sulfate shedding or protect against bleomycin-induced lung injury. However, experimental augmentation of airway heparanase activity significantly worsened post-bleomycin outcomes, confirming the importance of epithelial glycocalyx integrity to lung recovery. We hypothesized that MMP-associated heparan sulfate shedding contributed to delayed lung recovery, in part, by the release of large, highly sulfated fragments that sequestered lung-reparative growth factors such as hepatocyte growth factor. In vitro, heparan sulfate bound hepatocyte growth factor and attenuated growth factor signaling, suggesting that heparan sulfate shed into the air space after injury may directly impair lung repair. Accordingly, administration of exogenous heparan sulfate to mice after bleomycin injury increased the likelihood of death due to severe lung dysfunction. Together, our findings demonstrate that alveolar epithelial heparan sulfate shedding impedes lung recovery after bleomycin.

ARDS; glycocalyx; heparan sulfate; lung injury; lung repair

INTRODUCTION

First described by Ashbaugh and colleagues in 1967 (3), the acute respiratory distress syndrome (ARDS) is a critical illness characterized by disruption of the alveolar-capillary barrier, leading to pulmonary edema and hypoxemic respiratory failure. ARDS accounts for nearly a quarter of patients in intensive care units requiring mechanical ventilation and, despite advances in our clinical and scientific knowledge, continues to be associated with significant morbidity and mortality (4).

ARDS occurs in response to either direct injury to the pulmonary epithelium (e.g., pneumonia) or indirect injury to the lung via a systemic illness that damages the alveolar endothelium (e.g., nonpulmonary sepsis) (36). While direct and indirect insults induce lung injury via distinct pathogenic processes (9), both forms of injury are capable of damaging the glycocalyces of alveolar cells, leading to alveolar-capillary barrier dysfunction. The glycocalyx is an anionic matrix consisting of sulfated glycosaminoglycans anchored to the apical cell surface by membrane-bound proteoglycans (25). Indirect pulmonary insults cause lung injury by selectively damaging the glycocalyx of the alveolar endothelium (38), while direct pulmonary insults induce shedding of glycosaminoglycans from the alveolar epithelial surface (16). In a murine model of direct lung injury [intratracheal lipopolysaccharide (LPS)], we previously observed that matrix metalloproteinases (MMPs) rapidly cleaved epithelial glycocalyx proteoglycans, shedding full-length glycosaminoglycans such as heparan sulfate (HS) and chondroitin sulfate (CS) into the air space (16).

While MMPs have been long appreciated as key contributors to lung injury and repair, the dynamic control of MMP signaling is highly complex, being influenced not only by MMP expression but also by coexpression of endogenous inhibitors/activators of MMPs, as well as temporal shifts in these factors throughout the processes of injury onset and resolution (12). There exists remarkable structural and functional redundancy across different MMPs, as evidenced by the relative lack of MMP-selective pharmacological inhibitors (41). Furthermore, the biological impact of MMP signaling during lung injury can vary according to the cellular localization of MMP expression, with MMP9 expression from some cell types leading to lung injury (5) and expression of other MMPs leading to lung protection (6).

* W. B. LaRivière and S. Liao contributed equally to this work.
Correspondence: E. P. Schmidt (eric.schmidt@cuanschutz.edu).

Despite these complexities, MMPs have been extensively studied in the lung, commonly through the use of the bleomycin model of lung injury (7, 27, 45). However, little is known about the functional consequences of MMP-mediated pulmonary epithelial glycosaminoglycan shedding. The mechanisms responsible for this shedding are likely directly relevant to the processes of lung recovery, reflecting the potential influence of shed glycosaminoglycans on the local signaling environment. Full-length, negatively charged glycosaminoglycan polysaccharides are capable of sequestering positively charged proteins such as growth factors, thereby impacting downstream signaling pathways (19, 46). Accordingly, direct lung injury-induced glycosaminoglycan shedding into the air space may impede the availability of epithelial-reparative growth factors to the alveolar surface, potentially impairing the pace and efficacy of lung recovery.

In this study we sought to determine the mechanisms underlying alveolar epithelial glycocalyx shedding and their impact on lung recovery after intratracheal bleomycin, an insult that produces an early inflammatory response followed by a prolonged period of recovery amenable to experimental manipulation. We hypothesized that MMP-mediated shedding of air space HS sequesters lung-reparative growth factors such as hepatocyte growth factor (HGF) (20, 43, 48), impeding alveolar recovery after bleomycin exposure.

METHODS

Materials

Bleomycin (Enzo Life Sciences, Farmingdale, NY) was dissolved in phosphate-buffered saline (PBS) and stored at 4°C. Heparinase I/III from *Flavobacterium heparinum* (Millipore-Sigma, St. Louis, MO) was reconstituted in PBS. Reconstituted enzymes were stored at 4°C and used within 2 wk of resuspension. For controls, heparinase I/III was heat-inactivated at 100°C for 10 min. The broad-spectrum MMP inhibitor doxycycline hyclate (Millipore-Sigma) was reconstituted in deionized water and stored at 4°C according to the manufacturer's instructions. MLE-12 murine pulmonary epithelial cells (American Type Culture Collection, Manassas, VA) were cultured and passaged according to the manufacturer's instructions and grown in HITES-supplemented DMEM culture medium (American Type Culture Collection) unless otherwise specified. Heparin and chondroitin sulfate (CS)-A were purchased from Galen Laboratory Supplies (North Haven, CT). Tamoxifen for in vivo transgenic approaches was purchased from Millipore-Sigma.

Animals

Experiments were approved by the University of Colorado Institutional Animal Care and Use Committee and conducted in accordance with the National Institutes of Health guidelines. Wild-type 8- to 12-wk-old male C57BL/6 mice (Jackson Laboratories, Bar Harbor, ME) were used for the experiments. To generate heparanase (HPSE) FLEx switch mice (39), *Hpse* (*Hpse*-FNF-Tom-TK) embryonic stem cell clones, created by the Gates Stem Cell Center Bioengineering Core at the University of Colorado Anschutz Medical Campus, were injected into blastocysts derived from C57BL/6 mice to produce chimeras. Transmitting chimeric mice were backcrossed to C57BL/6 mice to establish founder lines. Male and female $Hpse^{fl/wt}$ offspring were crossed to yield homozygous *Hpse* FLEx switch lines. The homozygous $Hpse^{fl/fl}$ line was backcrossed to B6.Cg-Ndor1$^{Tg(UBC-cre/ERT2)1Ejb/1J}$ to yield $Hpse^{fl/wt}$-UBC-Cre-ERT2$^{+/-}$ mice. These animals were backcrossed more than five generations to a C57BL/6 background, yielding experimental $Hpse^{fl/fl}$-UBC-Cre-ERT2$^{+/-}$ and control $Hpse^{fl/fl}$-UBC-Cre-ERT2$^{-/-}$ (i.e., no Cre recombinase) lines. The UBC-Cre-ERT2 line will only yield wild-type or hemizygous animals; therefore, male or female offspring from $Hpse^{fl/fl}$-UBC-Cre-ERT2$^{+/-}$ × $Hpse^{fl/fl}$-UBC-Cre-ERT2$^{-/-}$ cross were used in the subsequent studies. Genotype and tamoxifen-activated Cre recombination were confirmed by PCR using primers as indicated in Table 1.

Mouse Treatment and Respiratory Mechanics

Intratracheal bleomycin-induced lung injury mouse model. Mice were anesthetized with inhaled isoflurane, given a single weight-adjusted dose of intratracheal bleomycin (1.2 μg/g body wt), as previously described (28), and followed for 3, 7, 14, or 21 days.

Respiratory mechanics and sample collection. Mice were sedated via intraperitoneal ketamine (80–100 μg/g)-xylazine (7.5–16 μg/g). After surgical exposure and cannulation of the trachea, mice were paralyzed with succinylcholine (0.24 mg/kg) for 3 min and the cannula was connected to a ventilator (flexiVent, Scireq, Montreal, PQ, Canada) for pulmonary function testing, as previously described (33). Next, anesthetized mice were terminally exsanguinated via inferior vena cava venipuncture. Bronchoalveolar lavage (BAL) was performed by delivery of three serial lavages with 1 ml of ice-cold sterile PBS through the tracheal cannula. Total cell number in BAL fluid was measured via manual hemocytometry. The BAL fluid was then centrifuged at 1,200 rpm for 5 min, and the supernatant was collected for later use (i.e., quantification of BAL protein, HS/CS mass spectrometry, Western blotting, and gelatin zymography). The pellet was resuspended in 400 μL of PBS for BAL differential cell counts. The suspended cells were deposited on a glass slide via centrifugation at 600 rpm for 2 min (Cytospin, Thermo Fisher, Waltham, MA), and the slides were stained with the PROTOCOL Hema 3 staining kit (Fisher Scientific, Hampton, NH) for BAL differential cell counts. Neutrophils, monocytes, lymphocytes, and erythrocytes were later counted in five distinct fields of view. Finally, the right lung was resected and snap-frozen in liquid nitrogen for protein and RNA isolation, while the left lung was inflated with 1% low-melt agarose and fixed in 10% buffered formalin phosphate (Thermo Fisher Scientific, Waltham, MA) for paraffin embedding and histological analysis.

In vivo MMP inhibition. Mice were treated with intratracheal bleomycin as described above. Beginning 7 days after intratracheal bleomycin treatment, once-daily weight-adjusted (70 μg/g body wt) doses of doxycycline were administered via oral gavage for 14 days until the mice were euthanized (21 days after intratracheal bleomycin treatment). This dose of doxycycline has been demonstrated to be sufficient to inhibit MMP2 and MMP9 activity within the injured lung (13, 35). BAL, blood, and lung tissue samples were collected and processed as described above.

Intrabronchial administration of glycosaminoglycans or bacterial heparinase. To administer experimental agents directly to the distal airways (avoiding tracheal contact), we intrabronchially (28) administered glycosaminoglycans similar in size and sulfation to endogenous shed HS (full-length, highly *N*-sulfated heparin) or CS (highly 4-*O*-sulfated CS-A). Similarly, we administered active or heat-inactivated heparinase I/III via intrabronchial injection. As previously described, we adjusted the dosing of intrabronchial administration to provide 60% of volume to the larger right lung and 40% to the smaller left lung, ensuring more homogeneous distribution of agents across both lungs (28).

Purification, Quantification, and Size Measurement of HS from BAL Fluid

Isolation and purification of HS for size analysis. HS fragments were isolated from BAL fluid harvested from mice at multiple time points after intratracheal bleomycin, as previously described (16). Briefly, BAL fluid samples were concentrated via lyophilization, resuspended in a solution containing 10 mg/mL actinase E (Millipore-Sigma, St. Louis, MO) and digestion buffer (0.005 M Ca^{2+} acetate

Table 1. *PCR primers*

Primer	Gene Target	Primer Type	Sequence	Position	Amplicon Length, bp
Hpse-GT-F20	*Hpse* forward	Genotyping	GGA TTC CAA GGG TAG TTG CTT G	Hpse promoter	Wild type: 236
Hpse-GT-R20	Hpse reverse	Genotyping	CTC TGC CCA GGA TCT CAG GTA	Hpse 3′-UTR	Floxed: 348
oIMR7338	Ub-Cre WT forward	Genotyping	CTA GGC CAC AGA ATT GAA AGA	Internal positive control forward	324
oIMR7339	Ub-Cre WT reverse	Genotyping	GTA GGT GGA AAT TCT AGC ATC	Internal positive control reverse	
25285	Ub-Cre transgene forward	Genotyping	GAC GTC ACC CGT TCT GTT G	UBC promoter	475
oIMR9074	Ub-Cre transgene reverse	Genotyping	AGG CAA ATT TTG GTG TAC GG	Cre transgene	
Hpse RecombF Set 3	*Hpse* FLEx switch forward	Recombination	GCT GTG TGT GCT ATG TGA AAT G	Hpse promoter	2,381
Hpse RecombR Set 3	*Hpse* FLEx switch forward	Recombination	GGG AAG GAC AGC TTC TTG TAA T	tdTomato	
Housekeeping gene for MMP7 PCR	GAPDH (mouse)	RT-PCR gene expression	CCC ATC ACC ATC TTC CAG GAG C	Forward	473
Housekeeping gene for MMP7 PCR	GAPDH (mouse)	RT-PCR gene expression	CCA GTG AGC TTC CCG TTC AGC	Reverse	
MMP7*	MMP7, forward	RT-PCR gene expression	GTG AGG ACG CAG GAG TGA AC	Spans exons 4 and 5	
MMP7*	MMP7, reverse	RT-PCR gene expression	ACA GGT GCA GCT CAG GAA GG	3′-UTR exon 6	
Mm00461768	Hpse TaqMan	Hpse mRNA	Commercial	Exon boundary 1–2	88
Mm01208359	Hpse TaqMan	Hpse mRNA	Commercial	Exon boundary 7–8	80
Mm03302254	Ppia TaqMan	Cyclophilin mRNA	Commercial	Exon 5	77
Mm00439498	Mmp2	MMP2 mRNA	Commercial	Exon 2–3	62
Mm00442991	Mmp9	MMP9 mRNA	Commercial	Exon 12–13	76

Hpse, heparanase; MMP, matrix metalloproteinase; Ppia, cyclophilin A; UB, ubiquitin; UTR, untranslated region; WT, wild-type. *Data from Wilson et al. (44).

and 0.01 M Na^+ acetate, pH 7.5), and placed in a 55°C water bath for 48–72 h. Samples were then loaded and run through an Amicon 3,000-molecular weight cutoff (MWCO) column (Millipore-Sigma, St. Louis, MO) to remove cellular debris. Samples were lyophilized again and resuspended in 400 μL of 8 M urea-2% (wt/vol) CHAPS aqueous solution and run through a Vivapure Q Mini H cation-exchange column (Sartorius-Stedim Biotech GmbH, Goettingen, Germany), washed, and eluted in 16% NaCl. Eluate was loaded onto another Amicon 3,000-MWCO column and then washed three times with 400 μL of deionized water for desalting and concentration. For isolation of chondroitin sulfate, 350 μL of digestion buffer (50 mM ammonium acetate with 2 mM calcium chloride adjusted to pH 7.0) and 5 μL of dissolved chondroitinase ABC (provided by Dr. Robert Linhardt, Rensselaer Polytechnic Institute, Troy, NY) were added to the eluted samples. Samples were placed in a 37°C incubator and allowed to digest for 1 h. Finally, CS disaccharides were isolated using Amicon 3,000-MWCO columns, and HS fragments were concentrated via lyophilization in preparation for PAGE.

Size measurement. Polyacrylamide gels were assembled as previously described (1). Briefly, the resolving gel (22% acrylamide) was poured into the gel cast, overlaid with deionized water, and allowed to polymerize for 30 min. The water was removed, and the stacking gel was poured and allowed to polymerize. Purified, lyophilized HS from BAL fluid and commercially purchased synthetic HS oligosaccharides of known size (Galen Laboratory Supplies, North Haven, CT) were then mixed 1:1 with a 50% sucrose solution with phenol red and loaded into the gel. The gel was run at 100 V for 5 min and then at 200 V for 40–45 min. The gel was then removed from its cast and stained with Alcian blue for 5 min and washed overnight in deionized water. On the next day, the gel was washed in 50% methanol for 40 min, washed in water for 2 h, and then placed in a silver nitrate (Millipore-Sigma, St. Louis, MO) staining solution for 30 min. Thereafter, the gel was washed in deionized water and developed until bands were visible, at which point the reaction was terminated and the gel was imaged.

HPLC-mass spectrometry. Glycosaminoglycans isolated from BAL fluid were analyzed via HPLC-tandem mass spectrometry (MS/MS) with multiple-reaction monitoring, as previously described (40). To estimate the native concentration of HS and CS in the alveolar lining fluid, we uniformly multiplied the concentration of HS recovered in the BAL by 37.92, a correction factor derived from the concentration of urea in BAL fluid relative to urea concentration in whole blood, as measured in previous experiments (16).

Molecular Biology Analyses

Western blotting. We first used a bicinchoninic acid-based protein assay (Bio-Rad, Hercules, CA) according to the manufacturer's instructions to quantify BAL protein concentrations. BAL sample aliquots were adjusted to equal protein concentrations, mixed with 5× Laemmli buffer, and then heated to 100°C for 10 min. Two micrograms of total protein per sample were loaded into 4–20% gradient Criterion Tris·HCl gels (Bio-Rad), subjected to gel electrophoresis, and transferred to a polyvinylidene difluoride membrane. The membranes were blocked, stained for MMP2 (1:1,000 dilution; Abcam, Cambridge, MA) or ERK1/2 and phosphorylated (T202/Y204) ERK1/2 (1:1,000 dilution; Cell Signaling, Danvers, MA), and developed using enhanced chemiluminescence. The developed film was scanned, and band intensity was quantified by ImageJ.

Zymography. BAL MMP2 and MMP9 gelatinolytic activity was quantified by zymography. Equal volumes of BAL fluid were added to 4× Laemmli buffer without reducing agents and loaded on Novex 10% gelatin protein zymogram gels (Invitrogen, Carlsbad, CA). After electrophoresis, the gel was renatured, developed at 37°C overnight,

and stained for 1 h with Bio-Safe Coomassie G-250 stain (Bio-Rad). The gel was then scanned, and band intensity was quantified by ImageJ.

In vitro HGF signaling assay. To measure the effect of soluble HS on HGF-mediated cell signaling, immortalized MLE-12 mouse type II alveolar epithelial cells were grown to ~75% confluency in HITES-supplemented DMEM with 10% FBS. The medium was then aspirated and replaced with DMEM supplemented with 1% FBS to induce serum starvation. After 8 h, cells were treated with 10 ng/mL recombinant mouse HGF (Sigma-Millipore, St. Louis, MO) and 1 μg/mL full-length HS, chondroitin sulfate-A (CS-A), or 6-, 10-, or 20-saccharide-long (dp6, dp10, or dp20) synthetic HS oligomers (Galen Laboratory Supplies, North Haven, CT) for 30 min. The cells were then washed and collected in ice-cold radioimmunoprecipitation assay buffer for Western analysis.

Heparanase activity assay. The ELISA-based heparanase activity assay (Genway Biotech, San Diego, CA) was performed according to the manufacturer's instructions, as previously described (38).

Glycoarray. The ability of HGF to bind to different glycosaminoglycans was tested using a commercially available glycosaminoglycan binding array (Z Biotech, Aurora, CO) according to the manufacturer's instructions. Briefly, HGF (20 μg/mL) was applied to a slide onto which glycosaminoglycans (HS, CS, or hyaluronic acid) of different sizes were affixed. After 3 h of incubation, the washed slides were stained with an Alexa Fluor 555-conjugated anti-HGF polyclonal antibody (5 μg/mL; catalog no. bs-1025R-A555, Bioss Antibodies, Woburn, MA). Slides were then washed and imaged using a fluorescence microscope. Slides exposed to antibody alone served as a negative control.

Quantitative real-time PCR. Heparanase (*Hpse*) expression in *Hpse*$^{f/f}$ mice was measured via quantitative real-time PCR (qRT-PCR). Briefly, QIAzol and the RNeasy mini kit (Qiagen, Germantown, MD) were used, according to the manufacturer's instructions, to isolate RNA from whole lung tissue. cDNA was synthesized using the iScript cDNA synthesis kit (Bio-Rad). Quantitative RT-PCR was performed using TaqMan probes (Thermo Fisher, Waltham, MA) and the Applied Biosystems (Foster City, CA) 7300 real-time PCR system. Cyclophilin was used as a housekeeping gene, and data were analyzed using the $2^{-\Delta\Delta Ct}$ method, as described by others (29). Probes are described in Table 1 (44).

Statistical Analyses

All treatments were administered to mice randomized to control or treatment groups, and experiments were performed across multiple days (with contemporaneous controls) to account for any unanticipated temporal confounders. For comparisons of two groups across multiple time points, we performed mixed-effects modeling (as opposed to 2-way ANOVA), given unequal numbers of replicates per group. Single comparisons were performed using a Student's *t* test (if data were in a normal distribution) or the Mann-Whitney test (nonparametric data). Multiple comparisons were performed using one-way ANOVA (followed by a Holm-Sidak correction), provided that standard deviations were similar across groups as determined by either Brown-Forsythe or Bartlett testing. Results were deemed statistically significant if $P < 0.05$. Statistical testing was performed using Prism (GraphPad, San Diego, CA).

RESULTS

Intratracheal Bleomycin Induces Lung Injury and Glycosaminoglycan Shedding

We administered a single weight-based dose of intratracheal bleomycin (1.2 μg/g) to isoflurane-anesthetized C57BL/6 mice. After 3, 7, 14, or 21 days, we anesthetized the mice again and measured pulmonary function (inspiratory capacity and dynamic respiratory system compliance); then we terminally sedated the mice and collected bronchoalveolar lavage (BAL) fluid and lung tissues (Fig. 1*A*). Consistent with the well-

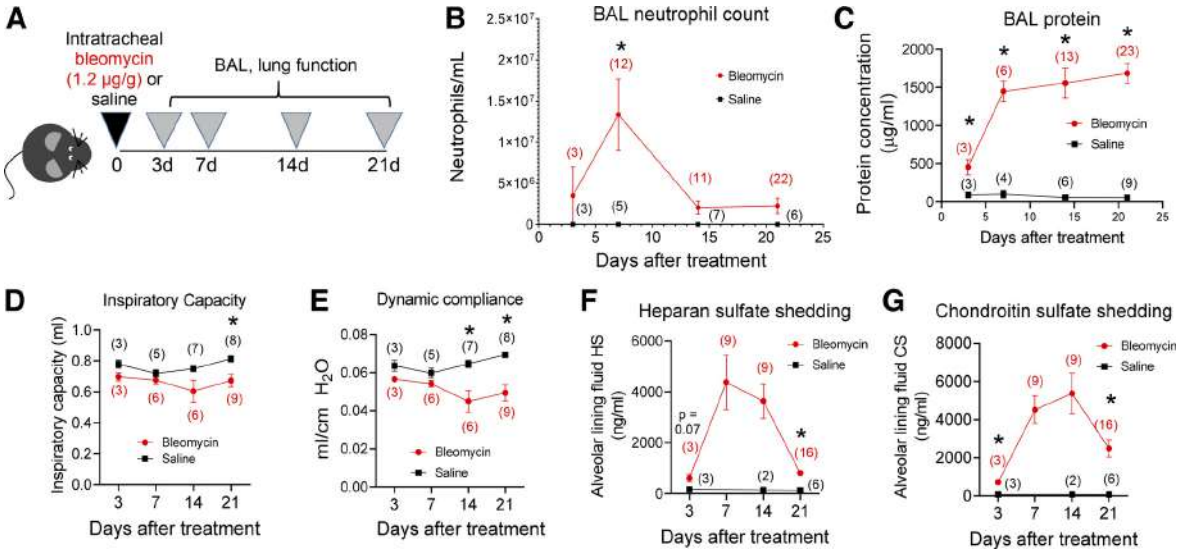

Fig. 1. Intratracheal bleomycin induces lung injury and glycosaminoglycan shedding. *A–C*: intratracheal bleomycin treatment (*A*) induced a neutrophilic alveolitis (*B*) with persistent elevations of bronchoalveolar lavage (BAL) fluid protein (*C*). *D* and *E*: pulmonary function testing revealed persistent impairment of inspiratory capacity (*D*) and dynamic compliance (*E*) in bleomycin-treated mice. *F* and *G*: bleomycin additionally induced persistent shedding of heparan sulfate (HS) and chondroitin sulfate (CS) into the air space, indicative of alveolar epithelial glycocalyx shedding. To guide later in vitro experiments, glycosaminoglycan (*F* and *G*) concentrations (measured by mass spectrometry) were corrected for BAL dilution (from pilot studies that determined a 38.97-fold dilution of BAL urea vs. blood urea) and reported as alveolar lining fluid concentrations. Numbers of experimental replicates are shown in parentheses for each data point. Given unequal numbers of replicates per group, mixed-effects analysis, as opposed to a 2-way ANOVA, was used for comparisons of bleomycin with saline over time; Holm-Sidak testing was used for multiple comparisons. *$P < 0.05$. For glycosaminoglycan analyses, testing was performed only on time points with >3 saline replicates. Error bars represent SE.

described injurious effects of bleomycin (32), we observed early (*day 7*) alveolar neutrophil influx (Fig. 1*B*) and persistent (*days 3, 7, 14*, and *21*) elevations in alveolar protein (Fig. 1*C*). As anticipated, this injury resulted in progressive impairment of lung physiology, as demonstrated by decreased inspiratory capacity and lung compliance (Fig. 1, *D* and *E*).

To determine the presence of alveolar epithelial glycocalyx shedding after bleomycin-induced lung injury, we used LC-MS/MS to measure the concentration of heparan sulfate (HS) and chondroitin sulfate (CS) in BAL fluid. To guide dosing for subsequent in vitro studies (as described in Fig. 6*E*) of the effects of HS and CS on epithelial growth factor signaling, we converted BAL concentrations of glycosaminoglycans to estimated alveolar lining fluid concentrations by correcting for BAL dilution, as determined by the ratio of BAL urea to blood urea calculated in pilot studies (16). We found that the onset of air space glycosaminoglycan shedding after intratracheal bleomycin coincided with neutrophil influx (*day 3*), peaked at 7–14 days, and persisted for ≥21 days after injury (Fig. 1, *F* and *G*). This prolonged shedding of HS and CS after intratracheal bleomycin is in contrast to the relatively brief (<5 days) shedding of alveolar glycosaminoglycans that we previously observed (16) after intratracheal LPS, a more rapidly resolving model of direct lung injury.

Bleomycin-Induced Glycosaminoglycan Shedding Is Mediated by MMPs and Impedes Lung Recovery

In a previous study (16) we determined that intratracheal LPS-induced shedding of alveolar HS was mediated by the MMP family of enzymes, which target proteoglycans that anchor HS and CS to the apical cell membrane (31). Consistent with these studies, we observed that intratracheal bleomycin similarly induced an increase of MMP2 in BAL fluid, as measured by Western blotting (Fig. 2*A*) and supported by gelatin zymography (Fig. 2*B*). Similarly, qRT-PCR of lung homogenates showed progressive induction of MMP2 (Fig. 2*C*) after bleomycin and only a transient (and not statistically significant) increase in MMP9 (Fig. 2*D*). RT-PCR conversely revealed only subtle induction of MMP7, which peaked at *day 21* (Supplemental Fig. S1, see https://doi.org/10.6084/m9.figshare.12137331.v1). Notably, induction of BAL MMP2 expression and activity correlated with the temporal course of air space HS shedding (Fig. 1). To determine if MMP family proteins were responsible for persistent alveolar glycosaminoglycan shedding after bleomycin, we administered daily doses of doxycycline hyclate (70 μg/g body wt), a broad-spectrum MMP inhibitor with known efficacy in vivo (35), by gavage (Fig. 2*E*) beginning 7 days after bleomycin. We elected to pursue this delayed approach to protease inhibition to avoid any confounding impact of doxycycline on the magnitude of the inciting lung injury, as well as to focus on the mechanisms responsible for persistent glycosaminoglycan shedding that may influence lung recovery after bleomycin. At 21 days after injury, delayed doxycycline treatment had no effect on BAL fluid protein levels (Fig. 2*F*) but attenuated cell surface HS shedding (Fig. 2*G*), suggesting that MMPs are responsible for mediating bleomycin-induced HS shedding. There was a nonsignificant attenuation of CS shedding (Fig. 2*H*), potentially suggesting that doxycycline-sensitive proteases preferentially targeted proteoglycans predominantly decorated with HS. Doxycycline treatment improved lung function 21 days after bleomycin (Fig. 2, *I* and *J*), suggesting that persistent induction of MMP activity impairs lung recovery, potentially by mediating the release of alveolar epithelial surface glycosaminoglycans into the air space.

Heparanase Is Upregulated in the Air Space After Bleomycin Treatment, But Does Not Impact Lung Recovery

While MMPs have been implicated as enzymes responsible for alveolar glycosaminoglycan and proteoglycan shedding after direct lung injury (16, 27), other modes of lung injury (e.g., sepsis-induced, "indirect" lung injury) may induce alternative "sheddases," such as heparanase, a HS-specific glucuronidase that directly degrades HS polysaccharides on the cell surface as well as in the extracellular matrix (42). While we previously observed that heparanase was not responsible for air space HS shedding (16) or lung injury (34) in the intratracheal LPS model of direct lung injury, we sought to confirm that this glucuronidase did not contribute to bleomycin-induced HS shedding or lung injury. Surprisingly, we found that BAL fluid heparanase activity (Fig. 3*A*) and lung homogenate heparanase expression (Fig. 3*B*) were elevated after bleomycin, suggesting that heparanase may contribute to air space HS shedding after bleomycin. However, pharmacological inhibition of heparanase (150 μg of *N*-desulfated, re-*N*-acetylated heparin, administered subcutaneously 3 times/day beginning 7 days after bleomycin; Fig. 3*C*) had no impact on BAL protein (Fig. 3*D*) or lung function (Fig. 3, *E* and *F*), as measured 21 days after bleomycin.

Pharmacological inhibitors of heparanase (including *N*-desulfated, re-*N*-acetylated heparin) are HS-based and, thus, confound mass spectrometry quantification of HS shedding. To determine if heparanase indeed contributes to HS shedding after bleomycin, as well as to confirm the findings of our pharmacological approach to heparanase inhibition, we created a transgenic, inducible heparanase (*Hpse*) knockout mouse. We used the FLEx switch approach (39) to establish a floxed heparanase mouse (C57BL/6 background), in which activation of Cre recombinase deletes exon 1 of *Hps*e and replaces it with a fluorescent marker (tdTomato) under the control of the endogenous heparanase promoter (Fig. 4*A*). We bred these mice to ubiquitin-Cre-ERT2 mice (C57BL/6 background, purchased from Jackson Laboratories), in which tamoxifen administration activates Cre recombinase in all tissues. As with our previously described pharmacological inhibitor experiments (Figs. 2*E* and 3*C*), we sought to antagonize heparanase expression after peak lung injury, thereby allowing us to study the effects of heparanase on lung recovery while avoiding any confounding attenuation of the inciting lung injury. We therefore administered daily tamoxifen intraperitoneally 7–11 days after bleomycin (Fig. 4*B*), an approach that led to successful recombination (Fig. 4*C*) and knockdown of heparanase expression (Fig. 4*D*) by *day 21*. Delayed heparanase knockdown again had no impact on BAL protein (Fig. 4*E*), alveolar HS shedding (Fig. 4*F*), or lung function (Fig. 4, *G* and *H*) 21 days after bleomycin.

The lack of impact of pharmacological or transgenic heparanase inhibition on HS shedding and lung function after bleomycin could reflect a relatively modest degree of endogenous heparanase induction within the air space of the lung.

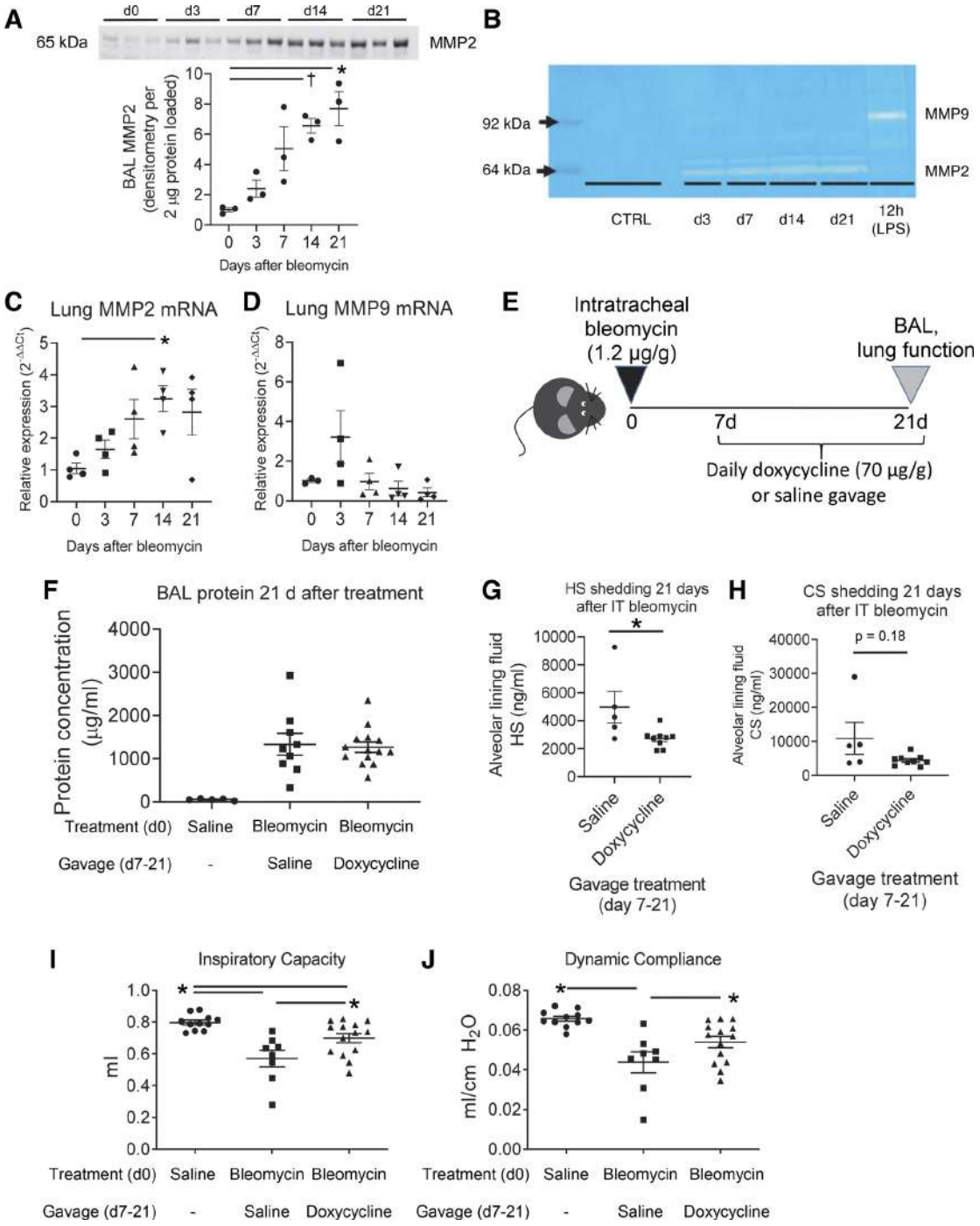

Fig. 2. Persistent activation of matrix metalloproteinases (MMPs) mediates ongoing shedding of heparan sulfate (HS) and lung dysfunction after bleomycin. *A* and *B*: intratracheal bleomycin treatment induces MMP2 expression (*A*; Western blot, 2 µg of protein loaded per well) and activity (*B*; gelatin zymography, 15 µL of fluid loaded per well) within bronchoalveolar lavage (BAL) fluid after bleomycin. CTRL, control; *d0, d3, d7, d14*, and *d21*, *days 0, 3, 7, 14*, and *21*. *C* and *D*: quantitative real-time PCR of whole lung homogenates from bleomycin-treated mice similarly demonstrates induction of MMP2 (*C*) but not MMP9 (*D*). *E–G*: inhibition of MMPs with doxycycline beginning 7 days after intratracheal (IT) bleomycin (*E*), a time course designed to avoid interference with the inciting lung injury, had no effect on BAL protein (*F*) but suppressed HS shedding (*G*) 21 days after bleomycin. Loss of HS shedding remained significant even if a single high-HS outlier in the saline group was excluded. *H*: doxycycline treatment induced a nonsignificant trend toward decreased chondroitin sulfate (CS) shedding 21 days after bleomycin. *I* and *J*: doxycycline treatment hastened lung recovery after intratracheal bleomycin, as shown by improved inspiratory capacity (*I*) and dynamic compliance (*J*). Mann-Whitney nonparametric testing was used for single comparisons (*G* and *H*); 1-way ANOVA with Holm-Sidak testing was used for multiple comparisons (*A–D, F, I*, and *J*). $*P < 0.05$, $\dagger P = 0.054$. Error bars represent SE.

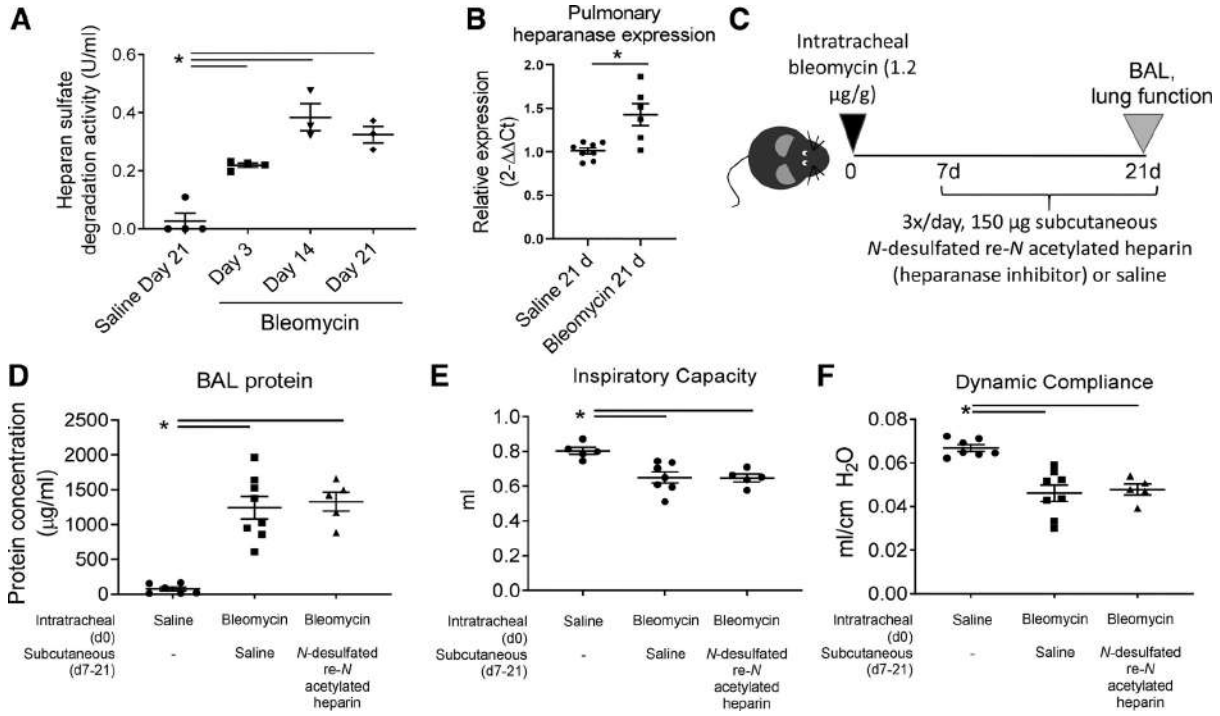

Fig. 3. Delayed pharmacological inhibition of heparanase does not improve pulmonary function after intratracheal bleomycin. *A* and *B*: intratracheal bleomycin treatment induces heparanase activity [*A*; in bronchoalveolar (BAL) lavage fluid] and expression (*B*; quantitative PCR in lung tissue) in C57BL/6 mice. *C*: to determine if delayed heparanase induction contributes to persistent pulmonary dysfunction after intratracheal bleomycin, we inhibited heparanase with subcutaneous injections (3 times/day) of *N*-desulfated, re-*N*-acetylated heparin beginning 7 days after intratracheal bleomycin, a time course designed to avoid interference with the inciting lung injury. *D–F*: pharmacological heparanase inhibition had no effect on BAL protein (*D*), inspiratory capacity (*E*), or dynamic compliance (*F*). Mann-Whitney nonparametric testing was used for single comparisons (*B*); 1-way ANOVA with Holm-Sidak testing was used for multiple comparisons (*A, D, E*, and *F*). *$P < 0.05$. Error bars represent SE.

This would be consistent with the undetectable level of tdTomato expression in the lungs of our heparanase knockout/reporter mouse 21 days after bleomycin (data not shown), suggesting either rapid clearance of the fluorescent protein or lack of significant heparanase promoter activation [consistent with the modest 21-day increase in lung *Hpse* mRNA (Fig. 3*B*)]. We therefore sought to determine if pharmacological augmentation of HS degradation within the distal air spaces would increase alveolar HS shedding and impair lung recovery after bleomycin. At 10–16 days after bleomycin, we administered bacterial heparinase I and III [which specifically degrade HS (38)] to both lungs by direct intrabronchial installation (Fig. 5*A*) at a dose sufficiently low to avoid persistent alveolar epithelial permeability in naïve lungs (16). Intrabronchial administration of low-dose heparinase I/III dramatically worsened outcomes after bleomycin (Fig. 5*B*). Mortality was defined by either death or moribund status, defined by lethargy and loss of >20% body weight, as measured by a blinded observer. All five mice receiving heparinase I/III after bleomycin progressed to meet moribund criteria; before euthanasia, these mice were anesthetized, and pulmonary function was tested and BAL was collected. These mice demonstrated elevated BAL protein (Fig. 5*C*), impaired lung function (Fig. 5, *D* and *E*), and neutrophilic alveolitis (Fig. 5*F*) compared with bleomycin mice treated with heat-inactivated heparinase I/III.

Together, our pharmacological and transgenic manipulations of heparanase indicate that endogenous induction of pulmonary heparanase after bleomycin is likely insufficient to mediate air space HS shedding or impede lung recovery. However, exogenous augmentation of HS degradation activity within the distal air spaces significantly worsened inflammatory lung injury and survival.

HS Fragments Shed After Bleomycin Impair Reparative Growth Factor Signaling In Vitro

While loss of the alveolar epithelial glycocalyx can induce local epithelial injury and alveolar dysfunction, the release of biologically active glycosaminoglycan fragments into the air space may also impact growth factor-mediated processes necessary for lung recovery (46). At 3–14 days after bleomycin, HS fragments released into the air space were >20 saccharides long (dp20) (Fig. 6*A*), a size sufficient to bind to HGF and other growth factors (48). By 21 days after bleomycin, HS fragment size had decreased independently of heparanase activity (Fig. 6*B*), further suggesting that endogenous heparanase exerts a minimal effect on air space glycosaminoglycans after intratracheal bleomycin. Air space HS fragments were highly sulfated at the amino (*N*-) position of glucosamine (Fig. 6*C*), another structural requirement necessary for HGF binding (48). Shed CS was largely 4-*O*-sulfated (30.95 ± 3.53% in saline controls and 69.61 ± 8.43% at *day 14*, $P < 0.05$, $n = 9–12$ per group), a sulfation pattern associated with minimal binding to HGF (48). Using a glycoarray approach, we confirmed our

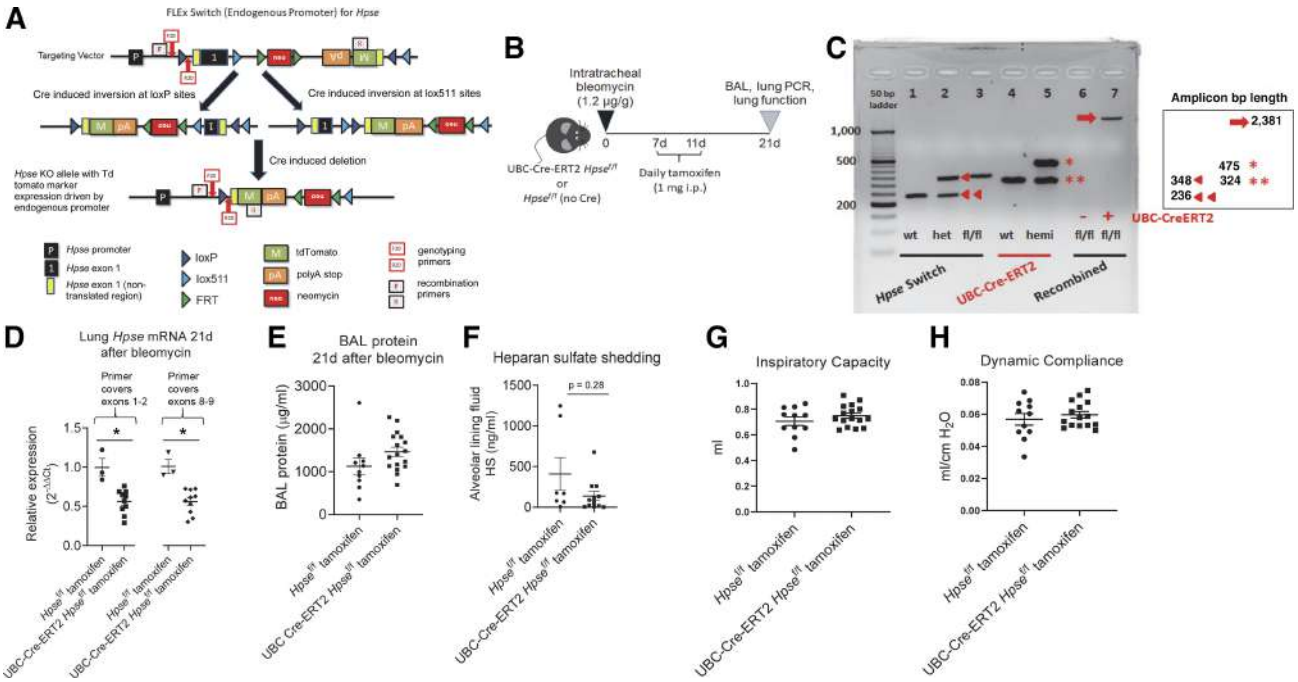

Fig. 4. Delayed, inducible global deletion of heparanase does not improve pulmonary function after intratracheal bleomycin. *A*: FLEx switch approach was used to create a genetic construct in which Cre recombinase excises exon 1 of heparanase (Hpse) and inserts a tdTomato reporter under control of the endogenous Hpse promoter. KO, knockout; FRT, Flp recombination target. *B*: to induce delayed loss of heparanase expression, we administered intratracheal bleomycin to mice that expressed tamoxifen-inducible Cre recombinase under the ubiquitin promoter (UBC-Cre-ERT2) and the floxed Hpse transgene (*Hpse$^{f/f}$*; genotyping shown in *C*) or mice expressing *Hpse$^{f/f}$* only (i.e., no Cre recombinase). BAL, bronchoalveolar lavage. *C* and *D*: beginning 7 days after bleomycin, we administered tamoxifen daily for 5 days to induce a delayed (*day 21*) loss of heparanase expression in the UBC-Cre-ERT2 *Hpse$^{f/f}$* mice, as demonstrated by genomic DNA recombination (*C*) as well as loss of heparanase mRNA (*D*) using primers at the site of recombination (exon 1) as well as distal to recombination (exons 8–9). *E–H*: delayed loss of heparanase had no effect on BAL protein (*E*), air space HS shedding (*F*), inspiratory capacity (*G*), or dynamic compliance (*H*) 21 days after bleomycin. Mann-Whitney nonparametric testing was used for single comparisons. *$P < 0.05$. Error bars represent SE.

previous surface plasmon resonance findings that HGF preferentially bound long (>dp20) *N*-sulfated heparins but not 4-*O*-sulfated CS (Fig. 6*D*). Low-level binding of HGF occurred with chondroitin sulfate D (>20 saccharide fragments), a 2-*O*-sulfated subtype of CS not enriched within post-bleomycin BAL.

To determine if HS binding to HGF impeded epithelial growth factor signaling, we treated MLE 12 cells (a mouse alveolar type II epithelial cell line) with HGF in the presence or absence of full-length *N*-sulfated HS. CS-A, which did not bind HGF, was used as a comparator glycosaminoglycan also shed into the air space after bleomycin. HGF induced ERK phosphorylation in MLE 12 cells, indicative of activation of epithelial growth factor signaling (Fig. 6*E*). This activation of growth factor signaling was inhibited by cotreatment with HS at concentrations relevant to the alveolar lining fluid in bleomycin-treated animals. Treatment with 4-*O*-sulfated CS had no impact on HGF-induced ERK phosphorylation.

Administration of Exogenous HS Increases the Risk of Lung Injury-Associated Mortality After Bleomycin

Given the results of our in vitro experiments, we sought to determine if air space HS, potentially via sequestration of proreparative epithelial growth factors such as HGF, is sufficient to impede lung recovery after bleomycin. We administered HS or CS to mice via bilateral intrabronchial injection 10 and 16 days after bleomycin (Fig. 7*A*). Administration of HS, but not CS, worsened survival after bleomycin (Fig. 7*B*). Of the five (out of 21) HS-treated mice that did not survive, four met our moribund criteria (as described above and assessed by a blinded observer) and were removed from the study. These four mice were anesthetized, subjected to pulmonary physiology assessment and BAL, and then euthanized under terminal sedation. No evidence of pulmonary hemorrhage was noted in any of the HS-treated mice, arguing against a heparin-like anticoagulant effect. Notably, there were no differences in overall BAL protein (Fig. 7*C*, also supporting the absence of bleeding), inspiratory capacity (Fig. 7*D*), or dynamic compliance (Fig. 7*E*) across all CS- or HS-treated bleomycin mice. However, when examined on an individual mouse level, HS-treated mice that progressed to moribund status demonstrated significant reductions in both inspiratory capacity (Fig. 7*D*) and dynamic compliance (Fig. 7*E*). These findings suggest that mice that did not survive the experiment died because of progressive respiratory failure. Together, these findings indicate that augmentation of air space HS increased the risk of death in the mice from progressive lung injury after bleomycin.

DISCUSSION

Consistent with our previous study (16), we found that direct lung injury caused shedding of the alveolar epithelial glycocalyx into the air space. However, in contrast with the LPS model of lung injury (16), bleomycin induced shedding that persisted well beyond the initial inflammatory injury and extended as

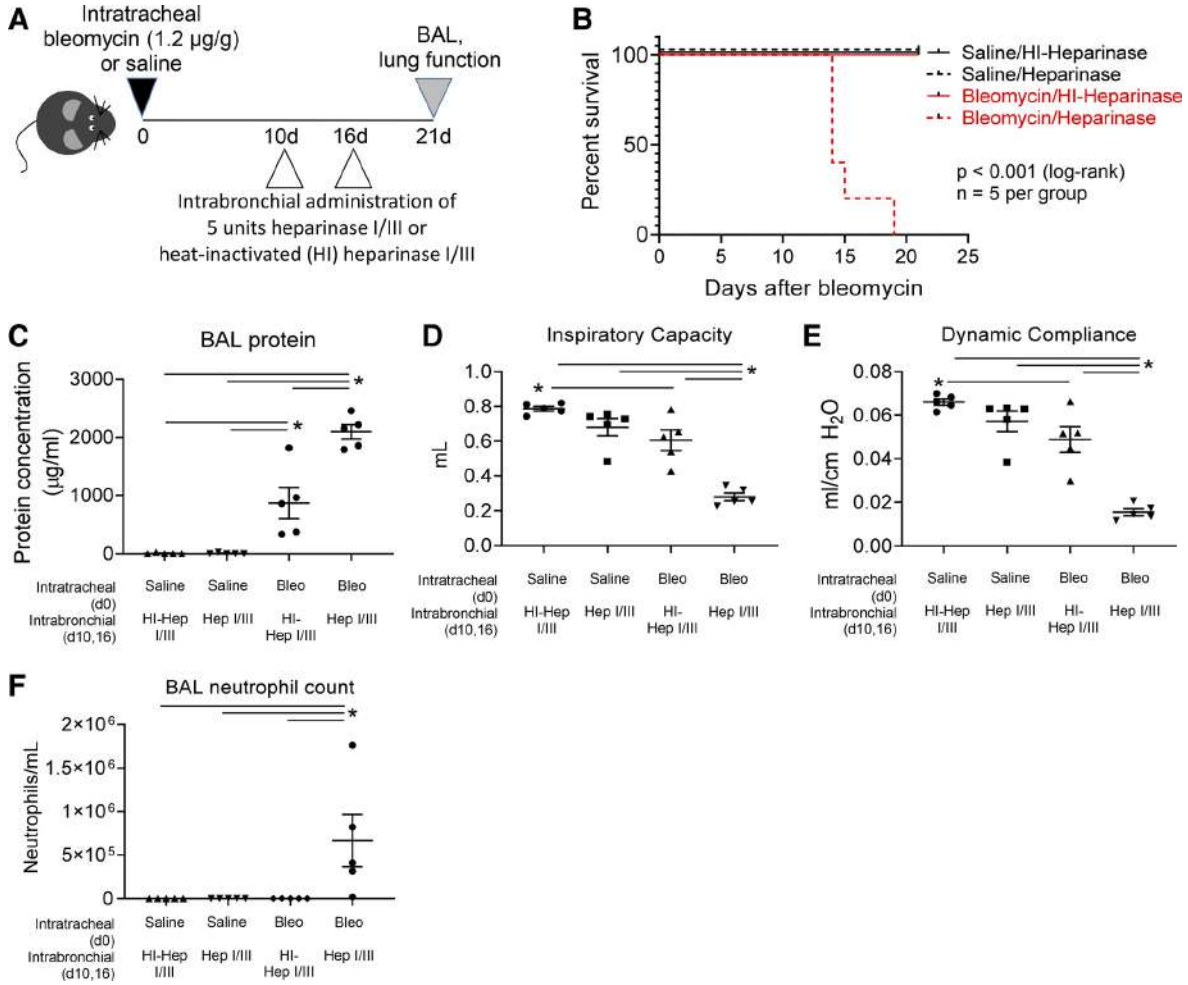

Fig. 5. Delayed, pharmacological augmentation of air space heparan sulfate (HS) degradation activity worsens bleomycin (Bleo)-induced lung injury. *A*: to augment air space HS degradation (i.e., heparanase) activity, a mixture of bacterial heparinase I/III (HepI/III; at a dose designed to avoid disruption of alveolar barrier function in control mice) was administered (via bilateral intrabronchial injection) 10 and 16 days after intratracheal bleomycin (or saline). Intrabronchial heat-inactivated (HI) heparinase I/III was administered as a control. *B*: active heparinase I/III induced mortality in bleomycin-treated mice (log-rank test), which met the moribund criteria as determined by a blinded observer. *C–F*: before euthanasia, heparinase I/III-treated mice demonstrated increased bronchoalveolar lavage (BAL) protein (*C*), decreased pulmonary function (*D* and *E*), and increased lung inflammation (*F*). Heat-inactivated heparinase I/III had no effect on either saline- or bleomycin-treated mice. One-way ANOVA with Holm-Sidak testing was used for multiple comparisons. $*P < 0.05$. Error bars represent SE.

long as 3 wk after treatment. Epithelial glycocalyx shedding coincided with a progressive induction of MMP2, and treatment with doxycycline (a nonselective MMP and protease inhibitor) beginning 7 days after injury reduced HS shedding and protected lung function. These findings suggest that MMPs may mediate ongoing HS shedding after bleomycin-induced lung injury and that attenuation of shedding is protective against the restrictive lung pathology that is a well-known feature of the bleomycin injury model.

MMPs have a well-described role in the pathogenesis of bleomycin lung injury (11, 23), largely as mediators of the fibrotic remodeling of the extracellular matrix (ECM). However, MMPs can influence other functions in the inflammatory response to injury, independent of fibrotic collagen deposition (15). MMP7 has been shown to mediate shedding of the HS proteoglycan syndecan-1, which promotes the alveolar influx of neutrophils during the inflammatory response to bleomycin injury (27). Furthermore, MMP7-induced shedding of E-cadherin attracts immunosuppressive leukocytes in the resolution phase of the injury response (30). While MMP2 is less well-studied than other members of the MMP family, it is known to be produced by alveolar epithelial cells, and its expression increases steadily over time after bleomycin treatment (24) and, along with MMP9 (10), has been shown to contribute to chemokine gradients that mediate the immunologic response to injury. While we did not observe significant induction of MMP7 (Supplemental Fig. S1) or MMP9 (Fig. 2*D*) in our model, we elected to broadly block all MMPs with the nonspecific inhibitor doxycycline, so as to avoid compensatory overexpression of MMPs that may occur in MMP-specific knockout mice (16). Other groups have shown a protective effect of doxycycline administered early after bleomycin (13), consistent with the known contributions of MMPs to the onset of lung injury. Our findings now demonstrate a protective

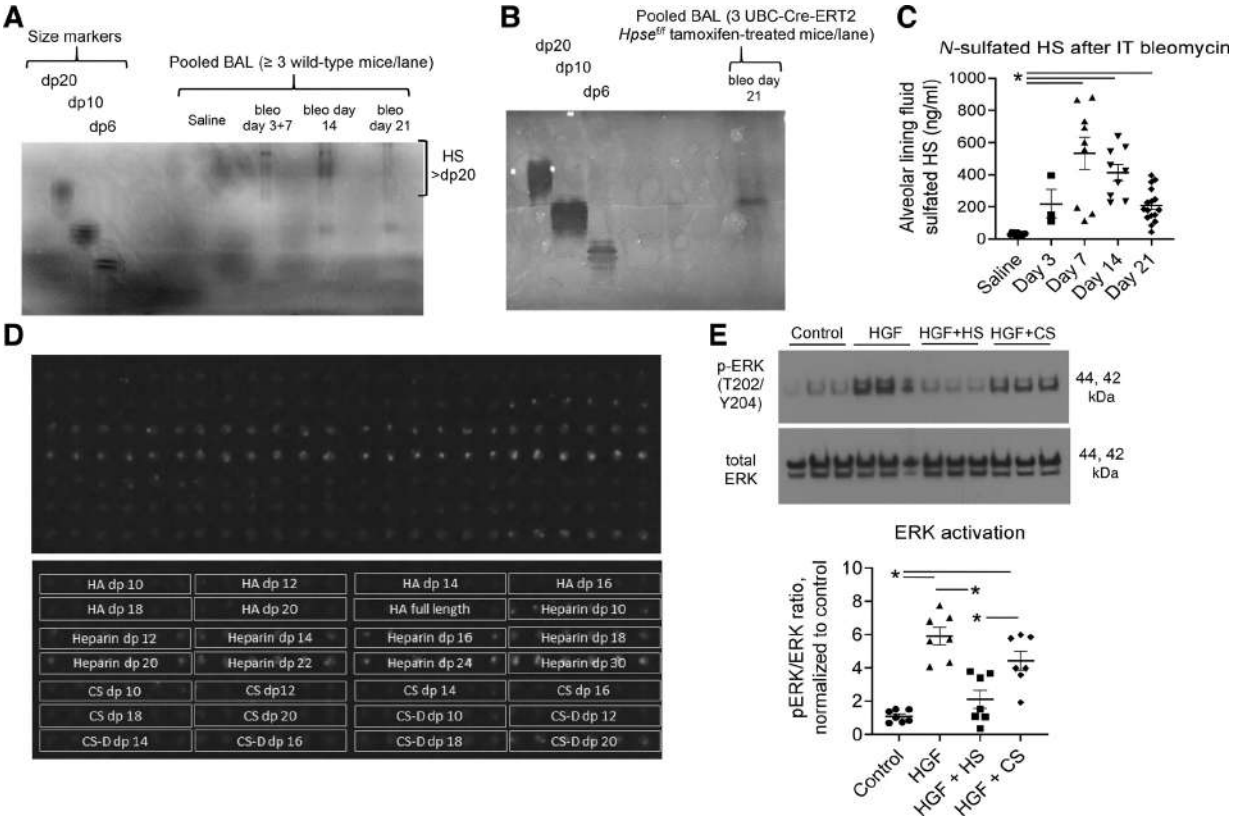

Fig. 6. Heparan sulfate (HS) fragments released into the air space after bleomycin (bleo) are of sufficient size and sulfation to bind and inhibit hepatocyte growth factor (HGF). *A*: PAGE reveals that HS fragments, released into the air space 3–14 days after bleomycin, are >20 saccharides long [degree of polymerization = 20 (dp20)]. *B*: at 14 and 21 days after bleomycin, HS fragment size decreases to ~dp10, a process that is independent of heparanase. Each lane represents ≥3 pooled samples. BAL, bronchoalveolar lavage. *C*: HS fragments shed after intratracheal (IT) bleomycin are highly sulfated at the amino position of glucosamine (*N*-sulfated), suggesting the ability to bind to positively charged residues of growth factors. *D*: glycoarray approaches confirm that HGF (representative of an epithelial-reparative growth factor) binds *N*-sulfated fragments as a function of HS length. Conversely, HGF does not bind hyaluronic acid (HA), chondroitin sulfate (CS), or 2-*O*-sulfated CS. *Top*: raw glycoarray image; *bottom*: annotated array image. *E*: concordant with the ability to bind HGF, HS (but not CS) impedes HGF-mediated activation of epithelial growth factor signaling, as measured by ERK phosphorylation (p-ERK). Experiments were repeated 3 times; 1 representative blot is shown. ANOVA with Holm-Sidak testing was used for multiple comparisons. $*P < 0.05$.

effect of a delayed initiation of doxycycline, even when administered after peak inflammatory injury. It is important, however, to note that the protective effects of doxycycline may be alternatively attributed to other doxycycline-sensitive proteases [such as a disintegrin and metalloproteinase (ADAM) family of proteases] (41), reflecting the broad ability of tetracycline antibiotics to chelate divalent cations (47). Indeed, the shared structural characteristics and functional redundancy of different MMPs, as well as similarities to ADAM family and aggrecanase proteases, have been a long-standing obstacle to the development of MMP-selective pharmacological inhibitors (41). Use of constitutive MMP2 knockout mice is similarly limited by abnormal pulmonary phenotypes (2, 18, 22), reflecting the importance of this MMP in lung development. Given these limitations, it is important to emphasize that our findings do not definitively prove a causal role for MMP2 as the mediator of bleomycin-induced alveolar HS shedding.

Regardless of the causal protease, persistent shedding of air space HS after lung injury may inhibit lung recovery via multiple mechanisms. We previously showed that the epithelial glycocalyx is necessary for maintenance of the alveolar barrier during lung homeostasis (16); accordingly, persistent degradation of the alveolar glycocalyx after bleomycin may delay recovery of normal alveolar-capillary integrity. However, persistent shedding of the cell surface glycocalyx can also release biologically active HS fragments capable of influencing growth factor signaling locally (46) and systemically (19). We found that bleomycin-induced epithelial glycocalyx degradation released long (>20 saccharides), highly sulfated HS fragments into the air space. Given that HS binding affinity for lung-reparative growth factors such as HGF (8, 14, 26) increases with HS fragment size and sulfation (48), the persistence of long, highly sulfated HS in the air space after bleomycin could lead to sequestration of HGF and other growth factors, impeding their availability to the recovering alveolar surface. Indeed, we found that highly *N*-sulfated, full-length HS fragments interfered with HGF activation of an alveolar type II epithelial cell line in vitro, providing mechanistic support for the hypothesis that air space HS fragments may sequester growth factors that contribute to lung repair. In further support of this hypothesis, intrabronchial administration of HGF-binding HS fragments after bleomycin increased the risk of progressive (and fatal) lung injury, while intrabronchial administration of non-HGF-binding CS had no deleterious effect on recovery after

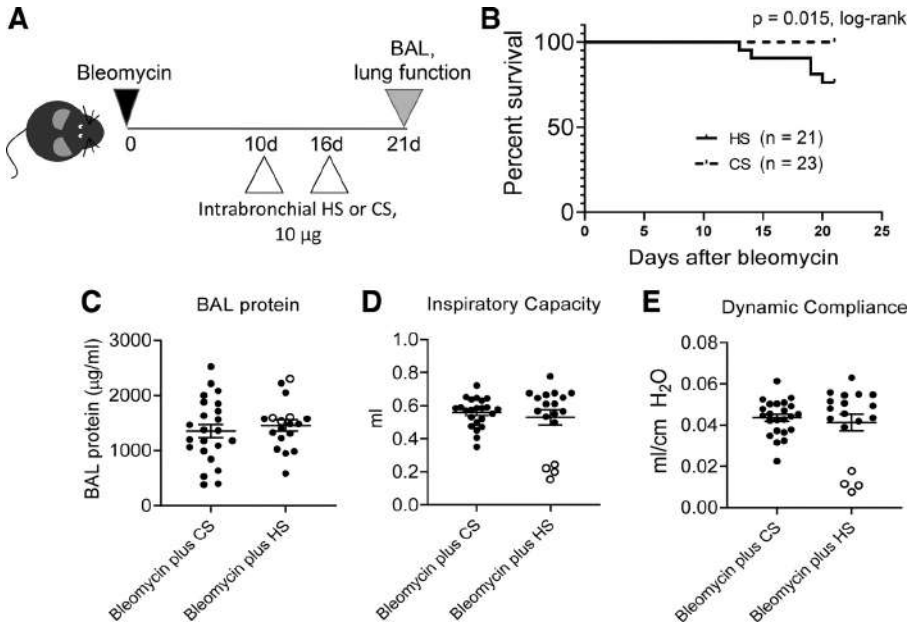

Fig. 7. Intrabronchial administration of full-length, highly *N*-sulfated heparan sulfate (HS) increases the risk of fatal lung injury after bleomycin. *A*: full-length, highly *N*-sulfated HS (heparin) or highly 4-sulfated chondroitin sulfate (CS-A) was administered via bilateral intrabronchial injection 10 and 16 days after bleomycin to determine if air space HS or CS is sufficient to worsen outcomes after intratracheal bleomycin. BAL, bronchoalveolar lavage. *B*: administration of exogenous HS, but not CS, increased the risk of mortality after bleomycin. Mortality was defined as death ($n = 1$) or meeting moribund criteria as determined by a blinded observer ($n = 4$). All surviving mice, as well as moribund mice before euthanasia, underwent terminal sedation and pulmonary function testing/BAL collection. *C–E*: while overall there were no differences in BAL protein or pulmonary function between mice randomized to HS or CS, HS-treated moribund mice (○) demonstrated profound reductions in pulmonary function (*D* and *E*), suggesting that exogenous HS increased the risk of progressive, fatal lung injury after bleomycin. Mann-Whitney testing was used for single comparisons; log-rank testing was used for survival analysis.

bleomycin. While the net sum of HS shedding appears to suppress reparative growth factor shedding, it is possible that a fraction of air space HS polysaccharides contains sulfation sequences that could potentially activate growth factor signaling, akin to heparin activation of anti-thrombin III or circulating HS activation of endothelial-reparative fibroblast growth factor 2 (46). Dissection of the individual sulfation patterns of shed alveolar HS and their sequence-dependent impact on alveolar function will require future mechanistic study (and the development of additional novel glycoanalytical technologies).

Our findings that bleomycin induces pulmonary MMPs (Fig. 2) concordant with the release of long, undegraded HS into the injured air space (Fig. 6) suggest that bleomycin induces expression of doxycycline-sensitive (Fig. 2) proteases that target the proteoglycans anchoring HS to the epithelial surface (and not HS itself). However, we (38) and others (17) previously demonstrated that nonpulmonary sepsis (an endothelial-targeted, indirect mode of lung injury) induces direct, heparanase-mediated cleavage of HS within pulmonary endothelial glycocalyx, leading to glycocalyx collapse and the release of degraded (octasaccharide) HS fragments into the circulation (37). Despite an increase in heparanase expression after bleomycin (Fig. 3), our pharmacological (Fig. 3) and transgenic (Fig. 4) studies indicate that this endogenous heparanase induction is not necessary for air space HS shedding after direct, alveolar epithelial-targeted modes of lung injury, corroborating previous studies of intratracheal LPS-induced injury (34). The absence of effect could suggest that the magnitude of endogenous heparanase induction within the air space after bleomycin was insufficient to induce pathogenically significant HS shedding. In support of this hypothesis, exogenously augmenting distal air space heparanase activity after bleomycin with intrabronchial administration of bacterial heparinases dramatically worsened injury. Together, these findings suggest a mechanistic compartmentalization of glycocalyx shedding (i.e., air space vs. intravascular) during lung injury and recovery.

Our study has several limitations in addition to the nonspecific inhibitory effects of doxycycline as discussed above. Our in vivo measures of outcome, pulmonary function, BAL fluid content, and all-cause mortality are incomplete reflections of the complex processes of recovery after lung injury. This is demonstrated in the discrepancy between the lung function and BAL fluid protein content in doxycycline-treated mice after bleomycin. While doxycycline attenuated HS shedding and improved lung restriction, it did not alter BAL fluid protein content compared with vehicle controls. However, this discrepancy may be consistent with previous studies of the bleomycin injury model (21) that suggest protein BAL fluid content is reflective of ongoing dysfunction of the alveolar-capillary barrier and is independent of bleomycin-induced restrictive lung disease. A further limitation is our focus on HGF as representative of all lung-reparative growth factors. As HS may electrostatically interact with numerous alveolar proteins, we cannot exclude disparate effects of HS shedding on other processes implicated in lung repair. Further studies to investigate the impact of HS and other shed glycosaminoglycans on the postinjury signaling environment are therefore warranted.

In conclusion, we found that bleomycin treatment causes protracted, protease (possibly MMP)-mediated shedding of the

pulmonary epithelial glycocalyx, leading to alveolar barrier dysfunction and impaired recovery from lung injury. These findings contrast with our previous study using the LPS injury model, in which acute injury leads to brief shedding of the alveolar glycocalyx and relatively rapid recovery. These shed HS fragments were biologically active and able to inhibit proreparative HGF signaling in vitro, suggesting that the prolonged shedding of glycocalyx HS may interfere with normal recovery from injury in the bleomycin mouse model. Furthermore, while endogenous induction of air space heparanase was insufficient to mediate persistent alveolar HS shedding or lung dysfunction after bleomycin, exogenous augmentation of distal air space heparanase activity significantly worsened post-bleomycin outcomes. These findings highlight the mechanistic importance of shed HS fragments to the pathogenesis of lung injury and may inform future efforts to improve therapeutic options for patients with ARDS.

ACKNOWLEDGMENTS

The authors thank the Genomics and Microarray Core at the University of Colorado Denver Anschutz Medical Campus for assistance with glycoarray analyses and the Gates Stem Cell Center Bioengineering Core at the University of Colorado Anschutz Medical Campus for assistance with creating the *Hpse*$^{fl/fl}$-UBC-Cre-ERT2$^{+/-}$ mice.

GRANTS

This project was funded by National Heart, Lung, and Blood Institute Grants F31 HL-143873-01 (to W. B. LaRivière) and R01 HL-125371 (to E. P. Schmidt and R. J. Linhardt) and Congressionally Directed Medical Research Program Grants W81XWH-18-1-0682 (to E. P. Schmidt and J. A. Bastarache) and W81XWH-17-1-0051 (to Y. Yang).

DISCLOSURES

No conflicts of interest, financial or otherwise, are declared by the authors.

AUTHOR CONTRIBUTIONS

W.B.L., J.A.B., E.P.S., and Y.Y. conceived and designed research; W.B.L., S.L., S.A.M., K.O., X.H., F.Z., S.Y., M.R., R.J.L., E.P.S., and Y.Y. performed experiments; W.B.L., S.L., S.A.M., K.O., X.H., F.Z., S.Y., M.R., R.J.L., E.P.S., and Y.Y. analyzed data; W.B.L., S.L., S.A.M., K.O., X.H., F.Z., S.Y., M.R., J.A.B., R.J.L., E.P.S., and Y.Y. interpreted results of experiments; E.P.S. prepared figures; E.P.S. drafted manuscript; W.B.L., K.O., X.H., J.A.B., E.P.S., and Y.Y. edited and revised manuscript; W.B.L., S.L., S.A.M., K.O., X.H., F.Z., S.Y., M.R., J.A.B., R.J.L., E.P.S., and Y.Y. approved final version of manuscript.

REFERENCES

1. **al-Hakim A, Linhardt RJ.** Electrophoresis and detection of nanogram quantities of exogenous and endogenous glycosaminoglycans in biological fluids. *Appl Theor Electrophor* 1: 305–312, 1991.
2. **Ambalavanan N, Nicola T, Li P, Bulger A, Murphy-Ullrich J, Oparil S, Chen Y-F.** Role of matrix metalloproteinase-2 in newborn mouse lungs under hypoxic conditions. *Pediatr Res* 63: 26–32, 2008. doi:10.1203/PDR.0b013e31815b690d.
3. **Ashbaugh DG, Bigelow DB, Petty TL, Levine BE.** Acute respiratory distress in adults. *Lancet* 290: 319–323, 1967. doi:10.1016/S0140-6736(67)90168-7.
4. **Bellani G, Laffey JG, Pham T, Fan E, Brochard L, Esteban A, Gattinoni L, van Haren F, Larsson A, McAuley DF, Ranieri M, Rubenfeld G, Thompson BT, Wrigge H, Slutsky AS, Pesenti A; LUNG SAFE Investigators; ESICM Trials Group.** Epidemiology, patterns of care, and mortality for patients with acute respiratory distress syndrome in intensive care units in 50 countries. *JAMA* 315: 788–800, 2016. [Erratum in *JAMA* 316: 350, 2016.] doi:10.1001/jama.2016.0291.
5. **Bradley LM, Douglass MF, Chatterjee D, Akira S, Baaten BJ.** Matrix metalloprotease 9 mediates neutrophil migration into the airways in response to influenza virus-induced Toll-like receptor signaling. *PLoS Pathog* 8: e1002641, 2012. doi:10.1371/journal.ppat.1002641.
6. **Cabrera S, Gaxiola M, Arreola JL, Ramírez R, Jara P, D'Armiento J, Richards T, Selman M, Pardo A.** Overexpression of MMP9 in macrophages attenuates pulmonary fibrosis induced by bleomycin. *Int J Biochem Cell Biol* 39: 2324–2338, 2007. doi:10.1016/j.biocel.2007.06.022.
7. **Cabrera S, Maciel M, Hernández-Barrientos D, Calyeca J, Gaxiola M, Selman M, Pardo A.** Delayed resolution of bleomycin-induced pulmonary fibrosis in absence of MMP13 (collagenase 3). *Am J Physiol Lung Cell Mol Physiol* 316: L961–L976, 2019. doi:10.1152/ajplung.00455.2017.
8. **Cahill EF, Kennelly H, Carty F, Mahon BP, English K.** Hepatocyte growth factor is required for mesenchymal stromal cell protection against bleomycin-induced pulmonary fibrosis. *Stem Cells Transl Med* 5: 1307–1318, 2016. doi:10.5966/sctm.2015-0337.
9. **Calfee CS, Janz DR, Bernard GR, May AK, Kangelaris KN, Matthay MA, Ware LB.** Distinct molecular phenotypes of direct vs indirect ARDS in single-center and multicenter studies. *Chest* 147: 1539–1548, 2015. doi:10.1378/chest.14-2454.
10. **Corry DB, Kiss A, Song LZ, Song L, Xu J, Lee SH, Werb Z, Kheradmand F.** Overlapping and independent contributions of MMP2 and MMP9 to lung allergic inflammatory cell egression through decreased CC chemokines. *FASEB J* 18: 995–997, 2004. doi:10.1096/fj.03-1412fje.
11. **Craig VJ, Zhang L, Hagood JS, Owen CA.** Matrix metalloproteinases as therapeutic targets for idiopathic pulmonary fibrosis. *Am J Respir Cell Mol Biol* 53: 585–600, 2015. doi:10.1165/rcmb.2015-0020TR.
12. **Davey A, McAuley DF, O'Kane CM.** Matrix metalloproteinases in acute lung injury: mediators of injury and drivers of repair. *Eur Respir J* 38: 959–970, 2011. doi:10.1183/09031936.00032111.
13. **Fujita M, Ye Q, Ouchi H, Harada E, Inoshima I, Kuwano K, Nakanishi Y.** Doxycycline attenuated pulmonary fibrosis induced by bleomycin in mice. *Antimicrob Agents Chemother* 50: 739–743, 2006. doi:10.1128/AAC.50.2.739-743.2006.
14. **Gazdhar A, Susuri N, Hostettler K, Gugger M, Knudsen L, Roth M, Ochs M, Geiser T.** HGF expressing stem cells in usual interstitial pneumonia originate from the bone marrow and are antifibrotic. *PLoS One* 8: e65453, 2013. doi:10.1371/journal.pone.0065453.
15. **Giannandrea M, Parks WC.** Diverse functions of matrix metalloproteinases during fibrosis. *Dis Model Mech* 7: 193–203, 2014. doi:10.1242/dmm.012062.
16. **Haeger SM, Liu X, Han X, McNeil JB, Oshima K, McMurtry SA, Yang Y, Ouyang Y, Zhang F, Nozik-Grayck E, Zemans RL, Tuder RM, Bastarache JA, Linhardt RJ, Schmidt EP.** Epithelial heparan sulfate contributes to alveolar barrier function and is shed during lung injury. *Am J Respir Cell Mol Biol* 59: 363–374, 2018. doi:10.1165/rcmb.2017-0428OC.
17. **Han S, Lee SJ, Kim KE, Lee HS, Oh N, Park I, Ko E, Oh SJ, Lee YS, Kim D, Lee S, Lee DH, Lee KH, Chae SY, Lee JH, Kim SJ, Kim HC, Kim S, Kim SH, Kim C, Nakaoka Y, He Y, Augustin HG, Hu J, Song PH, Kim YI, Kim P, Kim I, Koh GY.** Amelioration of sepsis by TIE2 activation-induced vascular protection. *Sci Transl Med* 8: 335ra55, 2016. doi:10.1126/scitranslmed.aad9260.
18. **Hendrix AY, Kheradmand F.** The role of matrix metalloproteinases in development, repair, and destruction of the lungs. *Prog Mol Biol Transl Sci* 148: 1–29, 2017. doi:10.1016/bs.pmbts.2017.04.004.
19. **Hippensteel JA, Anderson BJ, Orfila JE, McMurtry SA, Dietz RM, Su G, Ford JA, Oshima K, Yang Y, Zhang F, Han X, Yu Y, Liu J, Linhardt RJ, Meyer NJ, Herson PS, Schmidt EP.** Circulating heparan sulfate fragments mediate septic cognitive dysfunction. *J Clin Invest* 129: 1779–1784, 2019. doi:10.1172/JCI124485.
20. **Ito Y, Correll K, Schiel JA, Finigan JH, Prekeris R, Mason RJ.** Lung fibroblasts accelerate wound closure in human alveolar epithelial cells through hepatocyte growth factor/c-Met signaling. *Am J Physiol Lung Cell Mol Physiol* 307: L94–L105, 2014. doi:10.1152/ajplung.00233.2013.
21. **Jordana M, Dolovich M, Irving LB, Tomioka M, Befus D, Gauldie J, Newhouse MT.** Solute movement across the alveolar-capillary membrane after intratracheally administered bleomycin in rats. *Am Rev Respir Dis* 138: 96–100, 1988. doi:10.1164/ajrccm/138.1.96.
22. **Kheradmand F, Rishi K, Werb Z.** Signaling through the EGF receptor controls lung morphogenesis in part by regulating MT1-MMP-mediated activation of gelatinase A/MMP2. *J Cell Sci* 115: 839–848, 2002.
23. **Kim JY, Choeng HC, Ahn C, Cho SH.** Early and late changes of MMP-2 and MMP-9 in bleomycin-induced pulmonary fibrosis. *Yonsei Med J* 50: 68–77, 2009. doi:10.3349/ymj.2009.50.1.68.

24. **Kunugi S, Fukuda Y, Ishizaki M, Yamanaka N.** Role of MMP-2 in alveolar epithelial cell repair after bleomycin administration in rabbits. *Lab Invest* 81: 1309–1318, 2001. doi:10.1038/labinvest.3780344.
25. **LaRivière WB, Schmidt EP.** The pulmonary endothelial glycocalyx in ARDS: a critical role for heparan sulfate. *Curr Top Membr* 82: 33–52, 2018. doi:10.1016/bs.ctm.2018.08.005.
26. **Lee YJ, Moon C, Lee SH, Park HJ, Seoh JY, Cho MS, Kang JL.** Apoptotic cell instillation after bleomycin attenuates lung injury through hepatocyte growth factor induction. *Eur Respir J* 40: 424–435, 2012. doi:10.1183/09031936.00096711.
27. **Li Q, Park PW, Wilson CL, Parks WC.** Matrilysin shedding of syndecan-1 regulates chemokine mobilization and transepithelial efflux of neutrophils in acute lung injury. *Cell* 111: 635–646, 2002. doi:10.1016/S0092-8674(02)01079-6.
28. **Liao S, Eickelberg O, Schmidt EP, Yang Y.** Direct intrabronchial administration to improve the selective agent deposition within the mouse lung. *J Vis Exp* 20: 2019. doi:10.3791/59450.
29. **Livak KJ, Schmittgen TD.** Analysis of relative gene expression data using real-time quantitative PCR and the $2(-\Delta\Delta C_T)$ method. *Methods* 25: 402–408, 2001. doi:10.1006/meth.2001.1262.
30. **Manicone AM, Huizar I, McGuire JK.** Matrilysin (matrix metalloproteinase-7) regulates anti-inflammatory and antifibrotic pulmonary dendritic cells that express CD103 ($\alpha_E\beta_7$-integrin). *Am J Pathol* 175: 2319–2331, 2009. doi:10.2353/ajpath.2009.090101.
31. **Manon-Jensen T, Itoh Y, Couchman JR.** Proteoglycans in health and disease: the multiple roles of syndecan shedding. *FEBS J* 277: 3876–3889, 2010. doi:10.1111/j.1742-4658.2010.07798.x.
32. **Matute-Bello G, Frevert CW, Martin TR.** Animal models of acute lung injury. *Am J Physiol Lung Cell Mol Physiol* 295: L379–L399, 2008. doi:10.1152/ajplung.00010.2008.
33. **McGovern TK, Robichaud A, Fereydoonzad L, Schuessler TF, Martin JG.** Evaluation of respiratory system mechanics in mice using the forced oscillation technique. *J Vis Exp* 15: e50172, 2013. doi:10.3791/50172.
34. **Morris A, Wang B, Waern I, Venkatasamy R, Page C, Schmidt EP, Wernersson S, Li JP, Spina D.** The role of heparanase in pulmonary cell recruitment in response to an allergic but not non-allergic stimulus. *PLoS One* 10: e0127032, 2015. doi:10.1371/journal.pone.0127032.
35. **Ng HH, Narasaraju T, Phoon MC, Sim MK, Seet JE, Chow VT.** Doxycycline treatment attenuates acute lung injury in mice infected with virulent influenza H3N2 virus: involvement of matrix metalloproteinases. *Exp Mol Pathol* 92: 287–295, 2012. doi:10.1016/j.yexmp.2012.03.003.
36. **Ranieri VM, Rubenfeld GD, Thompson BT, Ferguson ND, Caldwell E, Fan E, Camporota L, Slutsky AS; ARDS Definition Task Force.** Acute respiratory distress syndrome: the Berlin definition. *JAMA* 307: 2526–2533, 2012.
37. **Schmidt EP, Li G, Li L, Fu L, Yang Y, Overdier KH, Douglas IS, Linhardt RJ.** The circulating glycosaminoglycan signature of respiratory failure in critically ill adults. *J Biol Chem* 289: 8194–8202, 2014. doi:10.1074/jbc.M113.539452.
38. **Schmidt EP, Yang Y, Janssen WJ, Gandjeva A, Perez MJ, Barthel L, Zemans RL, Bowman JC, Koyanagi DE, Yunt ZX, Smith LP, Cheng SS, Overdier KH, Thompson KR, Geraci MW, Douglas IS, Pearse DB, Tuder RM.** The pulmonary endothelial glycocalyx regulates neutrophil adhesion and lung injury during experimental sepsis. *Nat Med* 18: 1217–1223, 2012. doi:10.1038/nm.2843.
39. **Schnütgen F, Doerflinger N, Calléja C, Wendling O, Chambon P, Ghyselinck NB.** A directional strategy for monitoring Cre-mediated recombination at the cellular level in the mouse. *Nat Biotechnol* 21: 562–565, 2003. doi:10.1038/nbt811.
40. **Sun X, Li L, Overdier KH, Ammons LA, Douglas IS, Burlew CC, Zhang F, Schmidt EP, Chi L, Linhardt RJ.** Analysis of total human urinary glycosaminoglycan disaccharides by liquid chromatography-tandem mass spectrometry. *Anal Chem* 87: 6220–6227, 2015. doi:10.1021/acs.analchem.5b00913.
41. **Vandenbroucke RE, Libert C.** Is there new hope for therapeutic matrix metalloproteinase inhibition? *Nat Rev Drug Discov* 13: 904–927, 2014. doi:10.1038/nrd4390.
42. **Vlodavsky I, Friedmann Y, Elkin M, Aingorn H, Atzmon R, Ishai-Michaeli R, Bitan M, Pappo O, Peretz T, Michal I, Spector L, Pecker I.** Mammalian heparanase: gene cloning, expression and function in tumor progression and metastasis. *Nat Med* 5: 793–802, 1999. doi:10.1038/10518.
43. **Ware LB, Matthay MA.** Keratinocyte and hepatocyte growth factors in the lung: roles in lung development, inflammation, and repair. *Am J Physiol Lung Cell Mol Physiol* 282: L924–L940, 2002. doi:10.1152/ajplung.00439.2001.
44. **Wilson CL, Heppner KJ, Rudolph LA, Matrisian LM.** The metalloproteinase matrilysin is preferentially expressed by epithelial cells in a tissue-restricted pattern in the mouse. *Mol Biol Cell* 6: 851–869, 1995. doi:10.1091/mbc.6.7.851.
45. **Winkler MK, Fowlkes JL.** Metalloproteinase and growth factor interactions: do they play a role in pulmonary fibrosis? *Am J Physiol Lung Cell Mol Physiol* 283: L1–L11, 2002. doi:10.1152/ajplung.00489.2001.
46. **Yang Y, Haeger SM, Suflita MA, Zhang F, Dailey KL, Colbert JF, Ford JA, Picon MA, Stearman RS, Lin L, Liu X, Han X, Linhardt RJ, Schmidt EP.** Fibroblast growth factor signaling mediates pulmonary endothelial glycocalyx reconstitution. *Am J Respir Cell Mol Biol* 56: 727–737, 2017. doi:10.1165/rcmb.2016-0338OC.
47. **Zakeri B, Wright GD.** Chemical biology of tetracycline antibiotics. *Biochem Cell Biol* 86: 124–136, 2008. doi:10.1139/O08-002.
48. **Zhang F, Zheng L, Cheng S, Peng Y, Fu L, Zhang X, Linhardt RJ.** Comparison of the interactions of different growth factors and glycosaminoglycans. *Molecules* 24: 3360, 2019. doi:10.3390/molecules24183360.